THE JOURNAL OF BIOLOGICAL CHEMISTRY Vol. 278, No. 11, Issue of March 14, pp. 9885–9895, 2003
Printed in U.S.A.

Zinc Binding and Dimerization of *Streptococcus pyogenes* Pyrogenic Exotoxin C Are Not Essential for T-cell Stimulation*

Received for publication, July 11, 2002, and in revised form, December 4, 2002
Published, JBC Papers in Press, December 8, 2002, DOI 10.1074/jbc.M206957200

Wieslaw Swietnicki‡, Anne M. Barnie, Beverly K. Dyas, and Robert G. Ulrich§

From the United States Army Medical Research Institute of Infectious Diseases, Frederick, Maryland 21702

Streptococcal pyrogenic enterotoxin C (Spe-C) is a superantigen virulence factor produced by *Streptococcus pyogenes* that activates T-cells polyclonally. The biologically active form of Spe-C is thought to be a homodimer containing an essential zinc coordination site on each subunit, consisting of the residues His^{167}, His^{201}, and Asp^{203}. Crystallographic data suggested that receptor specificity is dependent on contacts between the zinc coordination site of Spe-C and the β-chain of the major histocompatibility complex type II (MHCII) molecule. Our results indicate that only a minor fraction of dimer is present at T-cell stimulatory concentrations of Spe-C following mutation of the unpaired side chain of cysteine at residue 27 to serine. Mutations of amino acid residues His^{167}, His^{201}, or Asp^{203} had only minor effects on protein stability but resulted in greatly diminished MHCII binding, as measured by surface plasmon resonance with isolated receptor/ligand pairs and flow cytometry with MHCII-expressing cells. However, with the exception of the mutants D203A and D203N, mutation of the zinc-binding site of Spe-C did not significantly impact T-cell activation. The mutation Y76A, located in a polar pocket conserved among most superantigens, resulted in significant loss of T-cell stimulation, although no effect was observed on the overall binding to human MHCII molecules, perhaps because of the masking of this lower affinity interaction by the dominant zinc-dependent binding. To a lesser extent, mutations of side chains found in a second conserved MHCII α-chain-binding site consisting of a hydrophobic surface loop decreased T-cell stimulation. Our results demonstrate that dimerization and zinc coordination are not essential for biological activity of Spe-C and suggest the contribution of an alternative MHCII binding mode to T-cell activation.

The 24.5-kDa Spe-C[1] protein is an exotoxin produced by the pathogenic bacterium *Streptococcus pyogenes*. Together with staphylococcal enterotoxin B (SEB), SEC, toxic shock syndrome toxin (TSST), and several others, Spe-C belongs to the superantigen protein family. Superantigens help pathogenic bacteria colonize the host by binding to major histocompatibility complex class II (MHCII) and T-cell receptors (TCR), thus bypassing the normal signal transduction pathway essential for immune recognition. In addition, the resulting nonspecific stimulation of the host's T-cells can induce pathological levels of cytokines. There is a substantial amount of structural data available for the superantigens, both free and in complex with their TCR and MHCII receptors (1–6). The superantigen fold is highly conserved despite low overall sequence similarity among protein family members. Superantigen-binding sites are found on the β-chain or on the α-chain of the MHCII receptor. The β-chain-binding site requires zinc to form a complex with the superantigen through a conserved His from MHCII and three His or Asp residues from the superantigen. The absence of zinc in certain superantigens, such as SEB, presumably precludes β-chain binding. The α-chain-binding site requires a structurally conserved positioning of a hydrophobic binding loop contributed by the superantigen, and usually a second polar binding pocket is also engaged. For the case of Spe-C, the α-chain binding loop is displaced, and the potential α-chain-binding site, if the Spe-C were to bind MHCII as a monomer, may be hidden in the interface of the zinc-dependent superantigen dimer (2), hypothetically resulting in interaction only with the MHCII β-chain. The β-chain binding residues are conserved in Spe-C and other streptococcal superantigens, and the β-chain-binding site (3, 4) is intact in crystallographic models in which this interaction site with MHCII critically involves zinc. Zinc was implicated in streptococcal superantigen binding to MHCII on the surface of cells (7–9), suggesting an essential role in both MHCII molecular recognition and TCR-mediated signal transduction. The high affinity zinc coordination complexes of SEA and Spe-C consist of three amino acid side chains contributed by the superantigen and the fourth by the MHCII receptor. As observed in structural data for the Spe-C tetrahedral zinc coordination complex (3–5), His and/or Asp contribute the zinc ligands from the superantigen and His^{81} from the β-chain of MHCII molecule. The recently determined crystal structure of SEH with the MHCII HLA-DR1 indicates a potentially lower affinity zinc coordination site, present at the interface with the receptor (6), where one of the ligands is a water molecule. The binding of SEH to MHCII is dependent on zinc, and superantigen potency is diminished when the zinc binding residues are replaced by alanines (10). However, the MHCII β-chain mutation H81A, expected to abolish the zinc-mediated SEH binding to MHCII, had minimal effect (10). In addition, the C-terminal zinc-binding site of another dimer-forming superantigen (11), SEC1, is not necessary for T-cell stimulation (12). *In vitro* data with purified recombinant Spe-C demonstrated a large proportion of dimer at 81 μM protein concentration (7), yet the K_d for

* The costs of publication of this article were defrayed in part by the payment of page charges. This article must therefore be hereby marked "*advertisement*" in accordance with 18 U.S.C. Section 1734 solely to indicate this fact.

‡ Senior fellow of the National Research Council. To whom correspondence may be addressed. Tel.: 301-619-4811; Fax: 301-619-2348; E-mail: wes.swietnicki@amedd.army.mil.

§ To whom correspondence may be addressed. Tel.: 301-619-4232; Fax: 301-619-2348; E-mail: ulrich@ncifcrf.gov.

[1] The abbreviations used are: Spe, streptococcal pyrogenic exotoxin; CDR, complementarity-determining region; FITC, fluorescein isothiocyanate; GdnHCl, guanidine hydrochloride; HLA, human leukocyte antigen; LB, Luria-Bertoni broth; LC-MS, liquid chromatography–mass spectrometry; MHCII, major histocompatibility complex type II; r wt, recombinant C27S mutant of Spe-C protein; SE, staphylococcal enterotoxin; TCR, T-cell receptor; TSST, toxic shock syndrome toxin; wt, wild type.

Report Documentation Page

Form Approved
OMB No. 0704-0188

1. REPORT DATE	2. REPORT TYPE	3. DATES COVERED
14 MAR 2003	**N/A**	**-**

4. TITLE AND SUBTITLE
Zinc binding and dimerization of Streptococcus pyogenes pyrogenic exotoxin C are not essential for T-cell stimulation, Journal of Biological Chemistry 278:9885 - 9895

5a. CONTRACT NUMBER
5b. GRANT NUMBER
5c. PROGRAM ELEMENT NUMBER

6. AUTHOR(S)
Swietnicki, W Barnie, AM Dyas, BK Ulrich, RG

5d. PROJECT NUMBER
5e. TASK NUMBER
5f. WORK UNIT NUMBER

7. PERFORMING ORGANIZATION NAME(S) AND ADDRESS(ES)
United States Army Medical Research Institute of Infectious Diseases, Fort Detrick, MD

8. PERFORMING ORGANIZATION REPORT NUMBER

9. SPONSORING/MONITORING AGENCY NAME(S) AND ADDRESS(ES)

10. SPONSOR/MONITOR'S ACRONYM(S)
11. SPONSOR/MONITOR'S REPORT NUMBER(S)

12. DISTRIBUTION/AVAILABILITY STATEMENT
Approved for public release, distribution unlimited

13. SUPPLEMENTARY NOTES
The original document contains color images.

14. ABSTRACT
Streptococcal pyrogenic enterotoxin C (Spe-C) is a superantigen virulence factor produced by Streptococcus pyogenes that activates T-cells polyclonally. The biologically active form of Spe-C is thought to be a homodimer containing an essential zinc coordination site on each subunit, consisting of the residues His(167), His(201), and Asp(203). Crystallographic data suggested that receptor specificity is dependent on contacts between the zinc coordination site of Spe-C and the beta-chain of the major histocompatibility complex type II (MHCII) molecule. Our results indicate that only a minor fraction of dimer is present at T-cell stimulatory concentrations of Spe-C following mutation of the unpaired side chain of cysteine at residue 27 to serine. Mutations of amino acid residues His(167), His(201), or Asp(203) had only minor effects on protein stability but resulted in greatly diminished MHCII binding, as measured by surface plasmon resonance with isolated receptor/ligand pairs and flow cytometry with MHCII-expressing cells. However, with the exception of the mutants D203A and D203N, mutation of the zinc-binding site of Spe-C did not significantly impact T-cell activation. The mutation Y76A, located in a polar pocket conserved among most superantigens, resulted in significant loss of T-cell stimulation, although no effect was observed on the overall binding to human MHCII molecules, perhaps because of the masking of this lower affinity interaction by the dominant zinc-dependent binding. To a lesser extent, mutations of side chains found in a second conserved MHCII alpha-chain-binding site consisting of a hydrophobic surface loop decreased T-cell stimulation. Our results demonstrate that dimerization and zinc coordination are not essential for biological activity of Spe-C and suggest the contribution of an alternative MHCII binding mode to T-cell activation.

15. SUBJECT TERMS
Streptococcus pyogenes, superatigen, pyrogenic exotoxin, receptor bining, zinc binding, superantigen

16. SECURITY CLASSIFICATION OF:			17. LIMITATION OF ABSTRACT	18. NUMBER OF PAGES	19a. NAME OF RESPONSIBLE PERSON
a. REPORT **unclassified**	b. ABSTRACT **unclassified**	c. THIS PAGE **unclassified**	**SAR**	**11**	

Standard Form 298 (Rev. 8-98)
Prescribed by ANSI Std Z39-18

dimer formation from equilibrium centrifugation data is only 390 μM (3) compared with T-cell stimulation occurring at nanomolar concentrations of superantigen. The mutant H35A, thought to affect dimer formation, had only minor effect on the K_d (3). Finally, the Spe-C molecule forms a zinc-less dimer in the Spe-C/TCR Vβ 2.1 crystal structure (13), using a surface proposed to be involved in the zinc-mediated MHCII binding, a site far removed from the one anticipated to bury the conserved residues interacting with the MHCII α-chain (2). Therefore, to further understand binding of Spe-C to MHCII and the contribution to T-cell stimulation, we have re-examined the relationship of zinc binding to stability, oligomerization, and biological function of the Spe-C superantigen. Our results suggest a diminished functional role for zinc and dimerization in T-cell stimulation. Further, an alternative zinc-independent-binding site, involving residues structurally equivalent to the MHCII α-chain-binding hydrophobic loop and polar pocket on SEB, may be biologically relevant for TCR stimulation. Binding to this site is only possible when the biologically active form of Spe-C is a monomer but not the homodimer.

MATERIALS AND METHODS

cDNA Cloning and Plasmid Construction—Genomic DNA was purified (Wizard Genomic DNA Isolation Kit; Promega) from a Spe-C$^+$ clinical isolate of *S. pyogenes* grown in a culture. The cDNA corresponding to the wt Spe-C was amplified by PCR and cloned into pRSET A vector between *Nhe*I and *Hin*dIII sites, together with a linker coding for a thrombin cleavage site (Leu-Val-Pro-Arg$_*$Gly-Ser) at the N terminus of Spe-C. The final construct coded for a fusion protein of His_6 (pRSET A vector) followed by a thrombin linker attached to the N terminus of mature Spe-C (amino acids 28–235). The protein construct was designed to have a Gly-Ser N-terminal extension after thrombin cleavage. To avoid covalent dimer formation because of an intermolecular disulfide bridge, a C27S mutation was introduced by site-directed mutagenesis (QuikChange; Stratagene). The full open reading frame corresponding to the fusion protein was sequenced on a CEQ 2000XL (Beckman, Fullerton, CA) sequencer. For protein expression, the plasmid DNA was transformed into a BL21 (DE3) strain (Invitrogen).

Protein Expression and Purification—A single colony from a freshly streaked LB + Amp (100 μg/ml) plate was grown in a 3 ml of LB + Amp (100 μg/ml) medium at 37 °C in a shaker for ~4 h until it became visibly turbid. A 0.5-ml aliquot was used to inoculate 25 ml of LB + Amp (100 μg/ml) medium and grown for an additional 4–5 h. The culture was then stored for 12 h at 4 °C. The next day, a 6-ml aliquot was added to 500 ml of LB + Amp (100 μg/ml) medium, and the culture was grown in a shaker at 37 °C until it reached A_{600} of 1.0. At that point, isopropyl-1-thio-β-D-galactopyranoside was added to a final concentration of 1 mM to induce protein expression, and the culture was grown overnight at 37 °C. Cells were harvested by centrifugation and stored at −80 °C until further processing.

To purify protein, bacterial cells from a 2-liter culture were thawed at room temperature and resuspended in ~120 ml of denaturing buffer (6 M GdnHCl, 100 mM potassium phosphate, 10 mM Tris-HCl, pH 8.0). Cells were disrupted by sonication on ice (3 × 1 min with a 1-min rest) using a Model 300 sonic dismembrator (Fisher Scientific, Hampton, NH) equipped with a ¼-in-diameter probe. Cellular debris was removed by centrifugation (2 h, 20,000 × *g*, 4 °C), and the supernatant was mixed with 25 ml of nickel-nitrilotriacetic acid Superflow resin (Qiagen) for 30 min to bind the protein. The resin suspension was used to pack a XK 26/20 column (Amersham Biosciences) in a batch mode, and the column was connected to a ÄKTA fast protein liquid chromatography system (Amersham Biosciences). Most cellular impurities were removed by washing with the denaturing buffer, and the protein was refolded by running a linear gradient of 100–0% of denaturing buffer and 100 mM potassium phosphate, 10 mM Tris-HCl, pH 8.0, over a 2-h time at a flow rate of 1 ml/min. Residual impurities were removed by a wash with 50 mM imidazole, 100 mM potassium phosphate, 10 mM Tris-HCl, pH 8.0, and the protein was eluted with 500 mM imidazole, 100 mM potassium phosphate, pH 5.8. The fractions containing protein, as judged by an SDS-PAGE analysis, were pooled and dialyzed against 10 mM Tris-HCl, 1 mM EDTA, pH 8.0. The His_6-thrombin linker was removed by digestion (20 °C, 7 d) with 10 units of thrombin (Amersham Biosciences) per mg of protein. The residual thrombin was removed by incubation with 1 ml of Q-Sepharose (Amersham Biosciences) resin, and the supernatant was dialyzed against 10 mM potassium phosphate, 1 mM EDTA, pH 5.8. The protein was bound to a SP-Sepharose (Amersham Biosciences) resin in a batch mode, and the suspension was used to pack a XK 26/20 column (Amersham Biosciences). The column was washed with 10 mM potassium phosphate, 1 mM EDTA, pH 5.8, buffer and developed with a linear gradient of 0–0.5 M NaCl at a 5 ml/min flow rate. Fractions containing protein, as judged by a SDS-PAGE analysis, were pooled and dialyzed against 10 mM HEPES, pH 7.0. The protein was concentrated in a Centriplus-3 (Millipore, Bedford, MA) concentrator, aliquoted, and stored at −80 °C. Protein concentration was determined by UV using molar extinction coefficients calculated with a ProtParam program on the ExPASy proteomics server at the Swiss Institute of Bioinformatics (Genève, Switzerland). Typically, 10–15 mg of purified protein at 0.5–2.5 mg/ml was obtained from 2L of bacterial cell culture. The purity of protein was verified by a combination of a SDS-PAGE and reversed-phase liquid chromatography. Proteins were characterized by LC-MS and, if needed, by an N-terminal amino acid sequencing. The final purity was greater than 95% as judged by LC-MS. The recombinant HLA-DR1 protein was prepared as described (24). The protein was stored in 20% glycerol at −20 °C at 5 mg/ml. A fresh aliquot was removed from the freezer and placed on ice directly before the experiments.

Mutant Construction and Purification—Mutants were constructed by site-directed mutagenesis (QuikChange; Stratagene). The full open reading frames corresponding to Spe-C fusion proteins were sequenced on CEQ 2000XL DNA sequencer (Beckman), and the plasmids were transformed into an *Escherichia coli* BL21 (DE3) strain for protein expression. Bacterial cell growth and protein purification were identical to the r wt protein (above). All mutant proteins contained the C27S replacement.

Metal Content Analysis—A protein sample volume corresponding to 0.5–1.0 mg of total protein was transferred to an empty sample container, weighed, and diluted to 5 ml with 2% nitric acid. The diluted sample was then analyzed by Hewlett Packard 4500 series inductively coupled plasma spectroscopy for zinc and nickel content. Detection limits for the method were 1 μg of metal per liter of solution.

LC-MS Analysis—The analysis was performed on a Finnigan LCQ Deca LC-MS. Typically, a 15-μl aliquot of protein solution was injected on a reversed-phase Poros II R/H 8 × 100-mm column (LC Packings, San Francisco, CA) equilibrated in 0.1% formic acid. The column was developed with a linear 0–100% gradient of 0.1% formic acid/80% acetonitrile over a period of 30 min at the flow rate of 0.250 ml/min. Eluent was also monitored at A_{280} on Agilent 1100 series UV-visible detector (Agilent Technologies, Palo Alto, CA). The data were stored on a computer and processed with the instrument's software.

Size Exclusion Chromatography—A total of 250 μl of protein solution at a concentration of 0.2 mg/ml in running buffer (100 mM potassium phosphate, 50 mM NaCl, pH 7.0) was injected onto Superdex 200 HR 10/30 (Amersham Biosciences) gel filtration column connected to a ÄKTA fast protein liquid chromatography system (Amersham Biosciences). Protein separation at the flow rate of 0.5 ml/min was monitored by following A_{280} of the eluent. The column was calibrated with gel chromatography markers (Amersham Biosciences). Molecular weight calculations of mutant Spe-C proteins were determined from plots of the logarithm of molecular weight of standards *versus* retention volume. All calculations assumed a globular shape of proteins.

Circular Dichroism Measurements—All measurements were made on a J-810 spectropolarimeter (Jasco, Inc., Easton, MD) equipped with a Peltier unit to control temperature of sample holding block. Unless otherwise specified, the block temperature was maintained at 25 °C. Far-UV spectra were collected in a 1-mm path length rectangular cuvette. Typically, at 0.2 mg/ml protein solution in 50 mM potassium phosphate, pH 7.0, data from ten spectra were collected and averaged. The spectra were corrected for the buffer, smoothed with programs included with the Jasco software, and converted to mean residue ellipticity, *MRE*, according to Equation 1, where Θ is the measured ellipticity in millidegree, c the protein concentration in mol/liter, d is the path length in cm, and N_a is the number of amino acid residues per molecule.

$$MRE = \frac{\Theta}{10cdN_a} \qquad \text{(Eq. 1)}$$

Secondary structure estimates were performed on the buffer-corrected, unconverted data with a Neural Network program from the Softsec program suite (Softwood Software).

Equilibrium unfolding experiments were performed with the Jasco

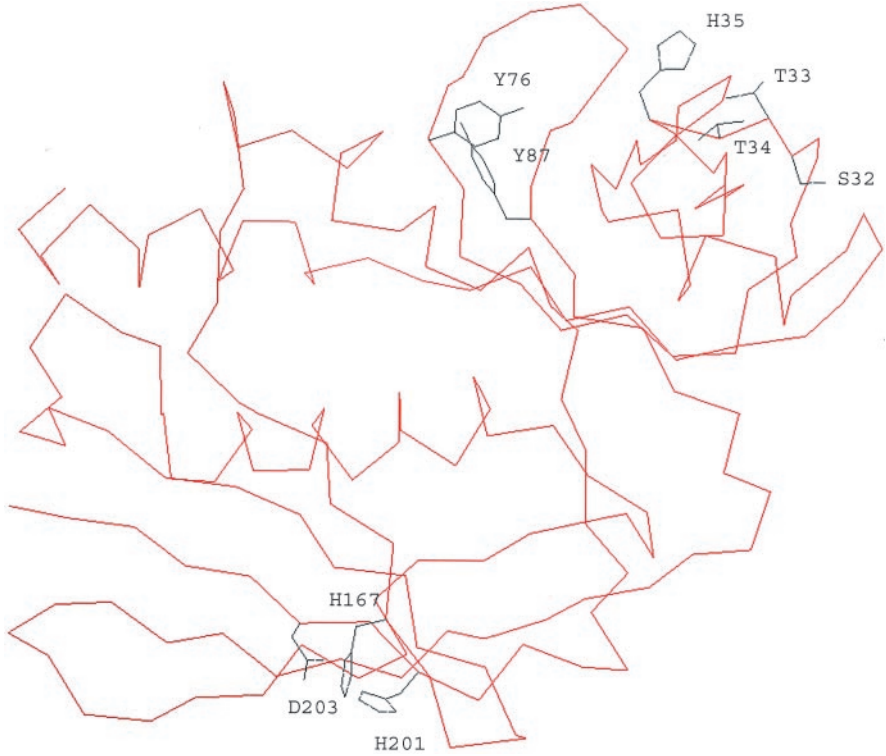

FIG. 1. **Residues of Spe-C mutagenized in the current work.** The zinc-binding site residues (*black*, *bottom left*) and the putative MHCII α-chain-binding site residues (*black*, *top right*) overlaid on the α-C backbone (*red*) of Spe-C are shown. The figure was generated with Swiss PDB Viewer v.3.7 (b2) (26).

titrator unit equipped with two 2.5-ml Hamilton syringes. Typically, about 10 ml of protein solution with concentration of 20 μg/ml in GdnHCl (5.4–5.6 M), 50 mM potassium phosphate, pH 7.0, was prepared, and about 2 ml was added in 50-μl increments to 2.7 ml of identical solution without GdnHCl in a 1-cm path length cuvette with constant mixing. The instrument and titrator parameters were as follows: titration steps, 40; mixing time after denaturant injection, 150 s; equilibration after solution withdrawal, 10 s; wavelength, 222 nm; response time, 8 s; average, two times; and bandwidth, 2 nm. Under these conditions, the signal recovery for refolding reaction was at least 90%. Data from unfolding were converted to ellipticity *versus* denaturant concentration by the Jasco software, transferred to Kaleidagraph program (Synergy Software, Reading, PA), and used for a non-linear fitting according to Equation 2, where Θ_{222} is the mean residue ellipticity at 222 nm, a is the slope, and b is the intercept of Θ *versus* denaturant concentration of the native, N, and unfolded, U, states, R is the gas constant equal to 8.315 J/mol M deg K, T is the temperature in K, m is the slope of ΔG *versus* denaturant concentration, c, and C_m is the concentration of denaturant at which 50% of the protein is unfolded.

$$\Theta_{222} = \frac{a_N + b_N c + (a_U + b_U c) exp\left(\frac{m(C_m - c)}{RT}\right)}{1 + exp\left(\frac{m(C_m - c)}{RT}\right)} \qquad \text{(Eq. 2)}$$

The free energy of unfolding at denaturant concentration equal to zero, ΔG^o, was calculated according to Equation 3.

$$\Delta G^o = mC_m \qquad \text{(Eq. 3)}$$

All measurements were made in duplicate or triplicate. Data are reported as means ± S.D. between independent measurements.

T-cell Proliferation Assay—Isolated human blood mononuclear cells were cultured for three days in 96-well plates (3–5 × 10^5 cells/well) in medium containing 5% fetal bovine serum (Invitrogen) and pulsed with 1 μCi of [^{3}H]thymidine (Amersham Biosciences) for a period of 9 h. SEA, SEB, and Spe-A were obtained from Toxin Technology, Inc. (Sarasota, FL). Cells were incubated in triplicate with bacterial toxins or recombinant Spe-C mutants and disrupted osmotically, and cellular debris was transferred to counting cassettes. Radioactivity was measured on a liquid scintillation counter (TopCount-NXT; Packard Instruments).

Endotoxin Level Determination—Endotoxin level measurements were measured by a Limulus-lysate assay (QCL-1000; BioWhittaker, Walkersville, MD). All protein samples had levels less than 0.24 endotoxin units/liter of solution.

Interactions of MHCII and Superantigens—Surface plasmon resonance measurements of ligand-receptor binding were performed on a Biacore 3000 (Biacore Inc., Piscataway, NJ). In a typical experiment, a solution of recombinant HLA-DR1 in 10 mM HEPES, pH 7.0, 150 mM NaCl was passed over a CM5 chip surface with immobilized superantigen (about 3000 refractive unit) at 20 μl/min for 3 min at 37 °C. The dissociation phase was followed for 2 min at the same flow rate, and the surface was regenerated with 10 mM EDTA and 2 M KCl. The sensogram was always corrected on a reference signal originating from a non-derivatized surface, measured in the same experiment. All data were processed for best fit using software supplied by the manufacturer and assuming a simple 1:1 Langmuire association model for the on-rate, k_{on}, off-rate, k_{off}, and dissociation constant, K_d, calculations. A cell-based MHCII binding assay was also used. The human B-lymphoblastoid cell line LG2 (16) was incubated with FITC-labeled r wt in Hanks' basic salt solution medium supplemented with 0.1% bovine serum albumin for 30 min at 37 °C. The cells were then washed with the medium, fixed with 1% paraformaldehyde in phosphate-buffered saline, and analyzed by a laser fluorescence-activated flow cytometry (BD Biosciences). Alternatively, mouse L cells expressing human DRα/DR1β (*B0101), prepared as previously described (11), were grown to 80% confluency. The cells were removed from tissue culture flasks with 25 mM EDTA in HBSS calcium- and magnesium-free medium, washed with Eagle's minimal essential medium supplemented with non-essential amino acids, and incubated with unlabeled r wt at the concentration range of 0.16-10 μM for 30 min at 37 °C. FITC-labeled r wt was then added to a final concentration of 1.25 μM, and the mixture was incubated for an additional 30 min at 37 °C. The cells were washed with Eagle's minimal essential medium, fixed with 1% paraformaldehyde in phosphate-buffered saline, and analyzed by laser fluorescence-activated flow cytometry (BD Biosciences).

Homology Modeling—Protein sequences were downloaded from a public data base through the PubMed program (National Library of Medicine). All models were constructed by Swiss Model program (26) on the ExPASy server at the Swiss Institute of Bioinformatics (Genève, Switzerland). The models optimized by the server and examined with the WHAT IF program (27) were either corrected manually or discarded if errors were too large. The crystallographic structure of SEH in complex with HLA-DR1 (6) was used to validate the homology modeling method. There was a high degree of correlation between modeled and experimental structures, presenting root mean square deviation of 0.4 and 1.0 Å for the α-C backbone of the superantigen alone and the whole complex, respectively.

TABLE I
A summary of mass determination data for Spe-C recombinant proteins

Spe-C	Molecular mass	Molecular mass
	exp. Da	*calc. Da*
r wt	24,481.2	24,478.3
D203A	24,437.4	24,434.3
H201A	24,415.3	24,412.2
H167A	24,416.7	24,412.2
D203N	24,480.3	24,477.3

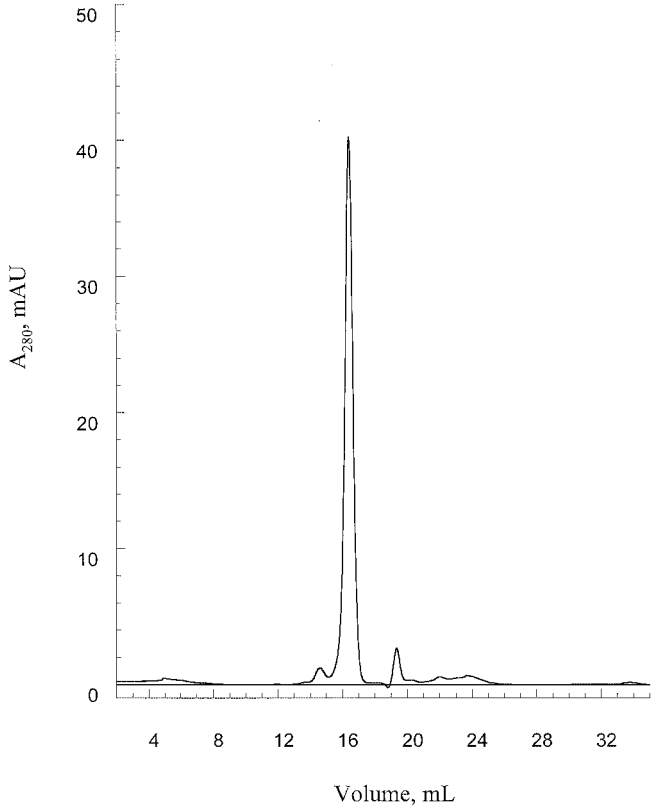

FIG. 2. **Gel filtration chromatography of recombinant H201A mutant at pH 7.0.** Traces for other proteins were similar and were excluded for clarity. The *small peak* at ~14.5 ml corresponds to dimer, and the *peak* at ~19.5 ml corresponds to the solvent. Protein concentration was 0.2 mg/ml.

TABLE II
Molecular weight determination of Spe-C mutants by size exclusion chromatography

Spe-C	Retention volume	Molecular mass	%	Oligomerization state
	ml	*calc. kDa*		
r wt	16.42	19.5	92.5	Monomer
	14.61	48.7	4.5	Dimer
	13.69	77.5	2.1	Trimer
H167A	16.4	19.7	97.3	Monomer
	14.57	49.9	2.4	Dimer
	13.98	66.7	0.2	Trimer
H201A	16.41	19.7	97.0	Monomer
	14.58	49.4	3.0	Dimer
D203A	16.45	19.3	98.3	Monomer
	14.78	44.7	1.5	Dimer
	13.58	81.5	0.2	Trimer
D203N	16.45	19.3	85.7	Monomer
	13.65	79.0	10.5	Trimer
	11.76	204	2.8	Oligomer

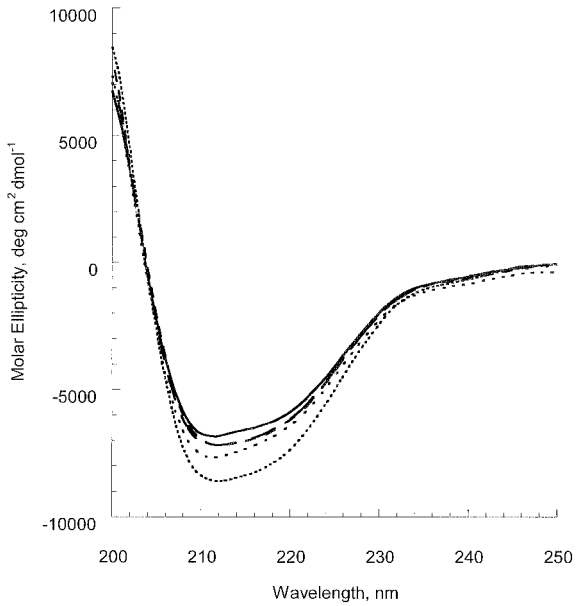

FIG. 3. **Far-UV circular dichroism spectra of recombinant wild type and mutant proteins.** *Solid line*, recombinant wild type; *short dots*, H201A; *long dots*, H167A; *long dash*, D203A; *short dash*, D203N. Protein solutions were prepared in 50 mM potassium phosphate, pH 7.0, at a concentration of 0.2 mg/ml.

Protein Docking—Molecular models were built with the Flexidock program in the Biopolymer module of Sybyl 6.7 (Tripos Software, St. Louis, MO) molecular modeling program suite. Starting templates were constructed by overlaying the α-C backbones of Spe-C on SEB from the SEB/DR1 complex (19). The Flexidock program uses a variation of a genetic algorithm (27) that employs a combination of rigid body and torsional space search. Final solutions are scored by the fitness function, which includes van der Waals, electrostatic, and torsional energy terms of the default Tripos force field, with the following modifications: hydrogen van der Waals radius, 1 Å; hydrogen bond epsilon, 0.03; and van der Waals cutoff distance for centroids, 16 Å. The strategy was used successfully for docking other proteins or small ligands (see Refs. 28–31). Because of the random nature of the genetic algorithm's initial search, we repeated all docking calculations for Spe-C. All solutions were the same as in the first simulation. Therefore, the structures presented represent converged, calculated structures. A typical run for docking of Spe-C or other superantigens to DR1 used default parameter settings with a 10-Å search radius around the starting binding pocket to maximize the search space. Contributions from electrostatics and all hydrogens were always included in the search parameters. A default initial seed number was used, but the total number of generations of Flexidock search was always limited to 3000 to avoid bias toward the best scoring solution. The following two approaches were selected for docking of Spe-C to DR1: 1) rigid body docking without flexing side chains; 2) all side chains of ligand and receptor were considered adjustable. Although the first strategy resulted in many solutions, all but one was considered unacceptable based on steric problems in the final models. The second strategy resulted in multiple solutions, which included, for most models, the residues structurally equivalent to the amino acids known to be critical for SEB binding to MHCII. The highest scoring solution from the second strategy was chosen for further optimization. The side-chain conformations for all residues were adjusted within the Biopolymer module, and the final models were energy-minimized with 20 steps of Simplex and 100 steps of a gradient (Pullman's method), using the Tripos force field (32).

To test the docking strategy, we built models of Spe-A/DR1, SEA/DR1, and SEC3/DR1 complexes. Analysis of the possible solutions revealed high scoring models, as judged by total energy and minimal steric problems, with potential binding residues that were structurally equivalent to SEB amino acids critical for MHCII binding. Predictions from the SEA/DR1 complex model were verified by previously published experimental data (16). Based on these test results, the strategy was assumed to be valid for searching for possible binding modes of Spe-C to DR1.

RESULTS

The Spe-C superantigen was cloned from a clinical isolate of *S. pyogenes*. r wt and mutants thought to be important for binding to MHCII molecules (Fig. 1) (discussed below) were

TABLE III
Thermodynamic parameters for equilibrium unfolding of Spe-C mutant proteins

Protein concentration was 0.817 μM in 50 mM potassium phosphate; pH 7.0. Thermodynamic parameter values are average ± S.E. of two-four independent measurements.

Spe-C	ΔG^o	C_m	m
	kJ/mol	*M*	*kJ/mol*$^{-1}$ *M*$^{-1}$
r wt	31.5 ± 2.1	1.16 ± 0.04	27.2 ± 2.6
H167A	30.6 ± 1.0	1.11 ± 0.04	27.7 ± 0.8
H201A	24.3 ± 2.9	0.92 ± 0.02	26.3 ± 2.6
D203A	26.5 ± 3.0	1.11 ± 0.02	23.8 ± 3.0
D203N	26.5 ± 2.2	1.14 ± 0.02	23.2 ± 1.4

TABLE IV
A summary of affinities of recombinant HLA-DR1 for Spe-C protein variants

The rate constants were determined at 37 °C in 10 mM HEPES; pH 7.0; 150 mM NaCl. The equilibrium dissociation constant for wt, determined from the plot of apex of the on-rates versus DR1 concentration; was between 1 and 2 μM. The value did not change when 10 mM potassium phosphate, pH 7.0, was used instead of the HEPES buffer. ND, not detected.

Protein	$k_{on} \cdot 10^3$	$k_{off} \cdot 10^{-3}$	K_d	$\Delta\Delta G^o$
	1/Ms	*1/s*	*μM*	*kJ/mol*
wt	2.74 ± 0.02	2.74 ± 0.12	1.0 ± 0.05	0
H167A	ND	ND	>50	>32
H201A	ND	ND	>50	>32
D203A	ND	ND	>50	>32
D203N	ND	ND	>50	>32

also constructed. To avoid dimerization because of covalent, intermolecular disulfide formation, all proteins had the mutation C27S introduced. The C27S mutation did not affect Spe-C biological function (discussed later) and allowed us to accurately measure the chemical stability and propensity to form a non-covalent dimer. Recombinant proteins were expressed in *E. coli* as inclusion bodies and refolded on-column under non-reducing conditions. The proteins were homogeneous as judged by SDS-PAGE (data not shown). Similar results were obtained when the mutants were analyzed by LC-MS, plotting the A_{280} and total ion current as a function of retention time (data not shown). The summary of mass assignments from LC-MS analysis is given in Table I. The experimental and calculated masses differ by less than four mass units, which excludes modifications due to post-translational modifications by *E. coli* and purification artifacts due to the refolding or chromatography procedures.

In view of reports indicating a possible dimer formation by the wt Spe-C, the recombinant proteins were analyzed by size-exclusion chromatography. A typical profile is shown in Fig. 2, and the experimental molecular masses of the main peaks are summarized in Table II. Assuming dissociation constant, K_d, of 0.390 mM for the dimer (3), the expected amount of monomer at 0.2 mg/ml (8.13 μM) protein concentration used in our size-exclusion chromatography experiments was about 97%. The slightly lower (93%; see Table II) proportion of the monomer may have been because of trimer formation, which was not included in our calculations. These results indicate that only a small population of dimer was present under our experimental conditions.

We next measured the far-UV circular dichroism spectra to characterize the quality of *in vitro* refolded recombinant proteins. The spectrum of r wt protein (Fig. 3) exhibits a minimum at 210 nm and a second, less pronounced minimum at about 220 nm. These data suggest a combination of α-helix and β-sheet as observed in the x-ray structure of Spe-C (2, 3). Estimates of secondary structure were as follows: 31% for α-helix, 21% for β-sheet, and 48% for coil. These experimental values, within the experimental error range, agree with the x-ray data (2, 3) as follows: 18 and 46% for the α-helix and β-sheet, respectively. The overall shape of the plots and absolute values of molar elliptically for the r wt protein are also very similar to the spectrum of the closely related Spe-A superantigen purified under non-denaturing conditions (14).

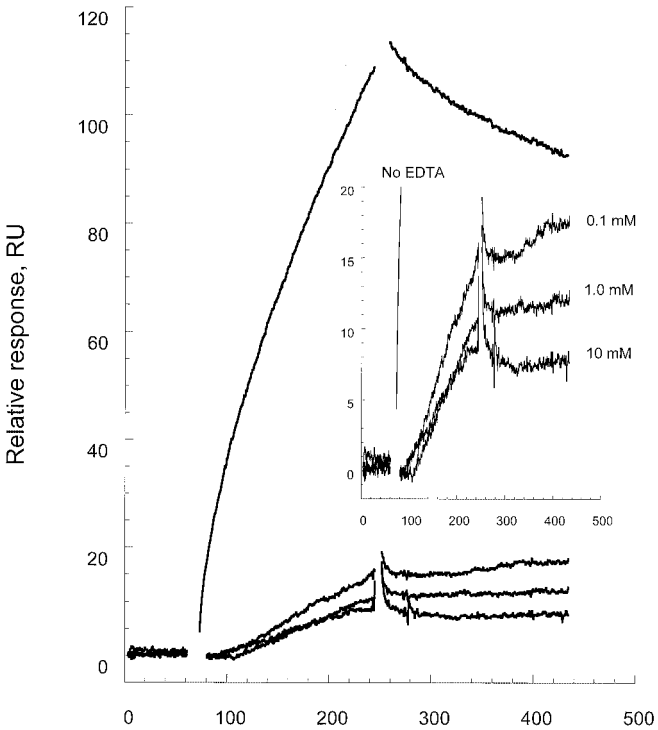

FIG. 4. **Chelation of divalent cations by EDTA dramatically reduces binding of HLA-DR1 to immobilized recombinant wild type Spe-C as measured by surface plasmon resonance.** *Main figure*, an overlay of all sensograms. *Inset*, a close-up of the binding sensograms in the presence of increasing concentration of EDTA (37 °C, 10 mM HEPES, pH 7.0, 150 mM NaCl). The HLA-DR1 concentration was 2 μM in all experiments to improve signal to noise ratio for sensograms in the presence of EDTA. For clarity, the data corresponding to start and end of the injection were removed from the graph. The *x* axis corresponds to time (s).

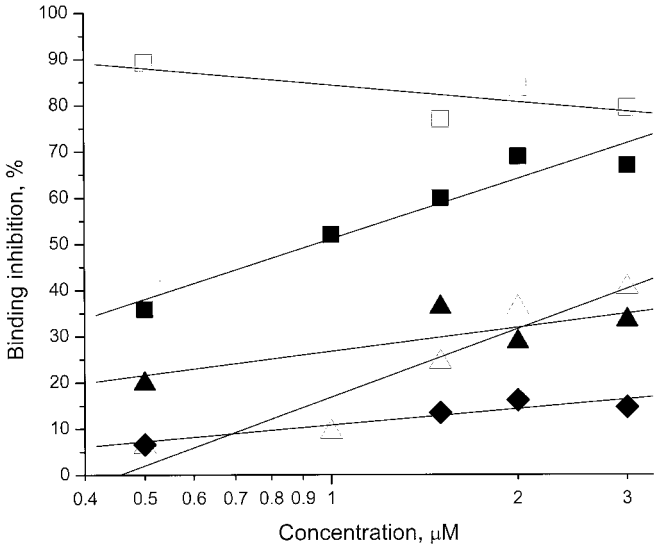

FIG. 5. **Competitive binding of recombinant Spe-C proteins to human LG2 cells.** □, recombinant wild type Spe-C; ▲, H167A; △, H201A; ♦, D203A; ■, D203N. Cells were incubated with a mixture of recombinant wild type Spe-C labeled with FITC and non-labeled Spe-C proteins. Receptor-bound fluorescence was measured by flow cytometry.

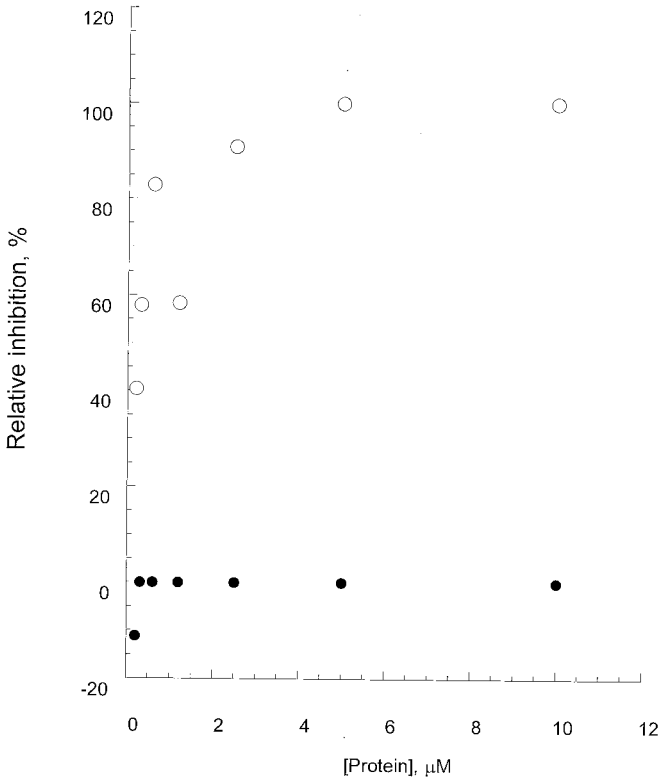

FIG. 6. **Wild type Spe-C binds exclusively to recombinant HLA-DR1 molecules expressed on the surface of cells.** Cells were incubated with a mixture of FITC-labeled recombinant wild type Spe-C and non-labeled competitor proteins. Receptor-bound fluorescence was measured by flow cytometry. ○, mouse L cells transfected with HLA-DR1; ●, non-transfected mouse L cells.

TABLE V
Zinc content of Spe-C proteins

Zinc content values are an average ± S.E. of at least two independent measurements. Nickel content was below the detection limit of the instrument. Under the experimental conditions, the minimum detectable metal content was 0.01–0.03 mole of metal/mole of protein.

Spe-C	Mole of zinc per mole of protein
r wt	0.11 ± 0.05
H167A	0.05 ± 0.01
H201A	0.06 ± 0.01
D203A	0.02 ± 0.01
D203N	0.20 ± 0.07

Based on the far-UV CD spectra of Spe-C mutant proteins, the secondary structure appeared to be similar to the r wt protein. However, the results for the H201A mutant may indicate potential folding problems in this protein. To further investigate, we measured the chemical stability of all recombinant proteins by GdnHCl unfolding. All proteins exhibited a cooperative transition under neutral pH conditions indicating a well folded species. The midpoint of transition, C_m, was 1.10–1.16 M for most proteins (Table III) and 0.92 M for the H201A mutant. The free energy of unfolding, ΔG^o, was 30–31 kJ/mol for the r wt and H167A mutant. The ΔG^o of the other mutants, however, were 24–26 kJ/mol. The differences, compared with r wt, were small but reproducible and may indicate that some of the zinc binding residues are important for protein stability.

Spe-C binding to soluble MHCII was measured by surface plasmon resonance, using HLA-DR1 expressed in S2 insect cells (24) and complexed with the influenza hemagglutinin peptide 306–318 (25). The r wt Spe-C bound HLA-DR1 with a dissociation constant of 1.0 μM whereas binding of zinc-binding

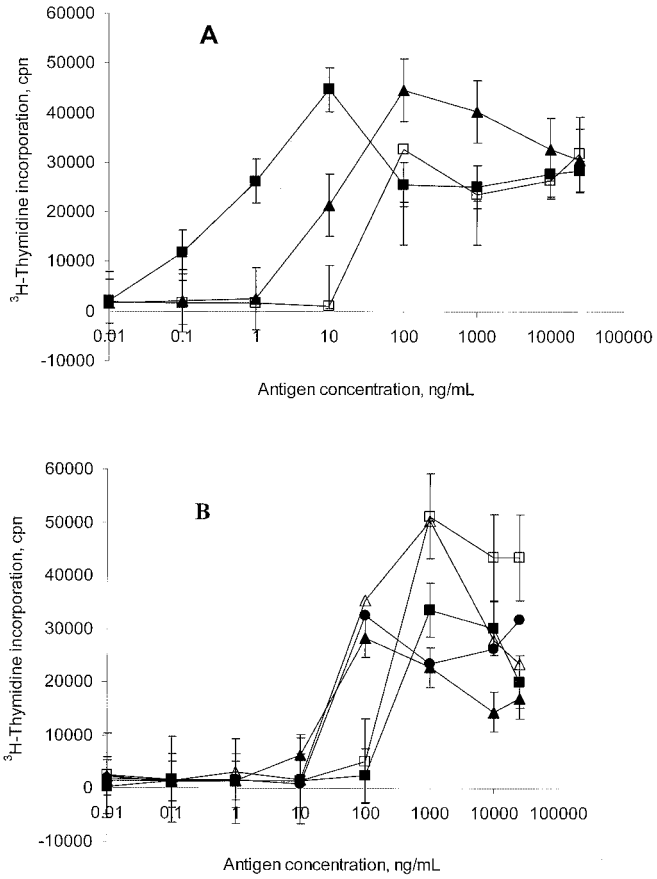

FIG. 7. **Human T-cell stimulation by Spe-C is not dependent on zinc.** *A*, wild type superantigens are shown as follows: □, wild type Spe-C; ■, wild type SEA; ▲, wild type Spe-A. *B*, recombinant Spe-C proteins are shown as follows: ●, wild type; ▲, H167A; △, H201A; ■, D203A; □, D203N.

site mutants was below the limits of detection (Table IV). Inclusion of EDTA in the analyte greatly inhibited binding (Fig. 4), suggesting zinc dependence. The residual binding (Fig. 4, *inset*) may indicate a secondary binding site on Spe-C for HLA-DR1. However, the signal was too weak to estimate the K_d reliably. We next measured the affinity of recombinant Spe-C mutants for MHCII molecules expressed on the cell surface to determine whether zinc was necessary for binding to the expressed receptors. All the Ala-substituted mutants of Spe-C had a significantly reduced affinity for the MHCII molecules expressed on LG2 cells (Fig. 5). The largest reduction was observed for the D203A mutant. Surprisingly, the affinity of the D203N mutant was five times greater than that of the r wt (K_d ~0.5 μM). The negative charge at position 203 was apparently not necessary for the MHCII binding.

To exclude the potential contribution to our binding data of HLA-DQ molecules co-expressed on the surface of LG2 cells, we performed binding studies with mouse L cells transfected with HLA-DR1 molecules. A representative result is shown in Fig. 6. Binding of the labeled r wt protein to the cell surface of HLA-DR1 transfected cells was blocked by adding increasing amounts of unlabeled Spe-C. The apparent K_i, determined as the concentration value at 50% of relative binding saturation, was 0.15 μM, a value lower than the K_i of 0.5 μM estimated from binding to human LG2 cells. The lower value may be because of the contribution of different sets of peptides bound by HLA-DR1 expressed on independent cell backgrounds. These results confirm that the binding data reflected direct interactions between HLA-DR1 and Spe-C. We concluded that the residues His^{167}, His^{201}, and Asp^{203} are important for binding to MHCII

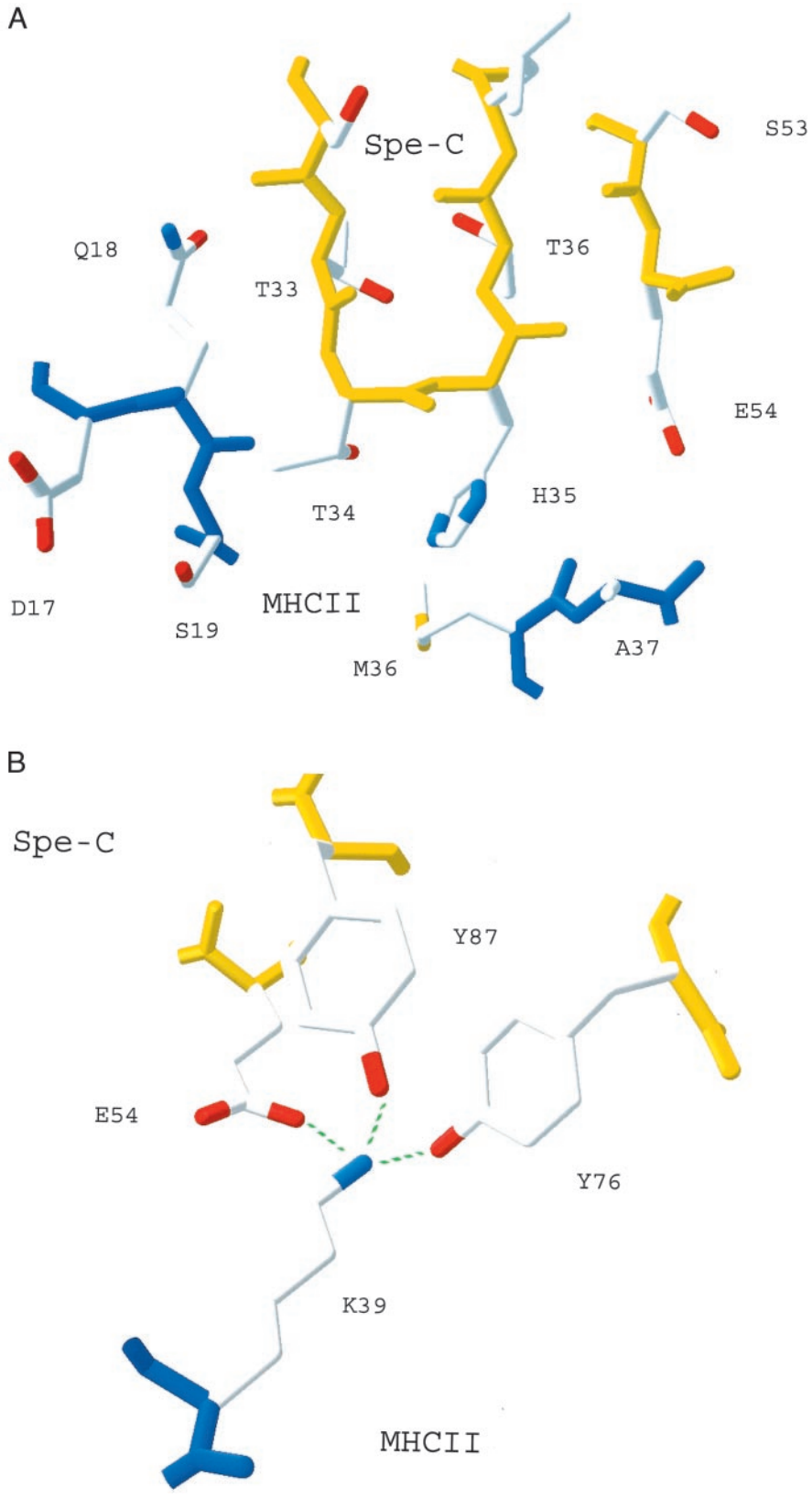

FIG. 8. **Close-ups of the hydrophobic loop (*A*) and polar pocket (*B*) regions in Spe-C proposed to bind HLA-DR1 α-chain.** The backbone atoms of DR1 and Spe-C are colored in *blue* and *yellow*, respectively. For clarity, only selected residues are shown.

molecules expressed on cells and in solution. Additionally, metal, most likely zinc, was essential for the overall binding of Spe-C to HLA-DR1, based on our metal content analysis (Table V) and cellular and surface plasmon resonance binding data. However, any potential secondary, zinc-independent MHCII-binding site was likely masked by the higher affinity, zinc-dependent site.

To investigate whether replacements in the zinc-binding site of Spe-C would affect the biological activity of the protein, we next measured human T-cell stimulation. The r wt protein was first compared with wild type SEA and Spe-A. SEA binds to the β-chain of MHCII molecules in a zinc-dependent mode and to the α-chain in a zinc-independent mode (15, 16), whereas the zinc-binding Spe-A has been proposed to bind only to the

α-chain (17). A typical T-cell stimulation assay for the wild type proteins is shown in Fig. 7*A*. The r wt superantigen produced by *E. coli* exhibits a typical superantigen response curve with $P_{50\%}$ ($P_{50\%}$ is defined as the concentration of antigen at which the T-cell stimulation is equal to half of the maximum T-cell response) between 10 and 100 ng/ml. The concentration of r wt toxin at which the response becomes saturated is also slightly higher than observed for the native SEA and Spe-A. To assess the importance of zinc-binding site for the T-cell stimulation potential of Spe-C, we next examined mutants of the zinc binding residues (Fig. 7*B*). The response point (the response point is defined by us as the lowest concentration of antigen at which the T-cell response is significantly higher than the baseline response) and $P_{50\%}$ values of the H167A mutant were identical to the wild type protein. The H201A mutant had the same response point, but the $P_{50\%}$ value was slightly higher. However, the response points of D203A and D203N mutants were higher than r wt values by an order of magnitude. The saturation values were equal or slightly higher than observed for the r wt protein. Clearly, none of the zinc-binding site mutations except at position 203 caused a dramatic decrease in biological activity. The replacement of Asp^{203} by either Ala or Asn caused a noticeable decrease in initial T-cell recognition. The T-cell response to the other mutants was essentially the same as obtained with the r wt protein. The difference between T-cell stimulation and MHCII binding by Spe-C may be a consequence of stabilizing interactions with cell surface proteins other than MHCII molecules (11). However, a major contribution by other proteins is unlikely in view of the experiments with the HLA-DR1 transfectants (Fig. 6) showing an exclusive binding to HLA-DR1. Although the Asp^{203} mutations resulted in only a slight change in protein-folding stability (Table III), we could not exclude the possibility that mutating this residue may perturb local secondary structure more than mutations in the other zinc-binding side chains. Collectively, these data suggest that zinc binding is not essential for T-cell recognition by Spe-C.

It is conceivable that in addition to the high affinity zinc-binding site observed in the crystal structure of Spe-C and MHCII complex (3), there may be a second, lower-affinity binding mode important for T-cell stimulation. We used protein docking simulations to facilitate a search for additional MHCII-binding sites in Spe-C that were zinc-independent. Several clusters of candidate binding sites were identified, generally close to the hydrophobic loop (discussed later). The final model structure, chosen based on the least amount of steric problems, was the solution most favored by the computational search. This solution also had the best agreement with our experimental data. The orientation of Spe-C *versus* DR1 in the modeled complex is very similar to the SEB/DR1 complex (root mean square deviation between the complexes is 0.53 Å for the α-C atoms). There are two major contact sites in the Spe-C/DR1 model complex: a hydrophobic loop (Fig. 8*A*), containing no intermolecular hydrogen bonds, and a polar pocket (Fig. 8*B*). Both sites form an almost continuous binding surface. The side chain of residue Thr^{34} from the hydrophobic loop packs very tightly against the peptide backbone of Ser^{19}-Gln^{18} from the α-chain of DR1. The polar pocket residue Tyr^{76} is on a flexible loop. This loop also contacts the following residues from the TCR Vβ 2.1 chain (13): Ile^{77} from the complementarity-determining region 2/frame-work region 3 (CDR2/FR3), Leu^{78} from CDR1, CDR2/FR3, and hypervariable 4/FR3 regions, and Asn^{79} from CDR1 and CDR3 regions of TCR Vβ 2.1. An overlay of our modeled DR1/Spe-C complex on the published Spe-C/TCR Vβ 2.1 complex crystal structure (13) revealed no steric clashes between HLA-DR1 and TCR Vβ, suggesting the likelihood of a ternary complex of Spe-C/MHCII/TCR based on this alternative binding mode. It should be noted that the zinc-binding site and hydrophobic loop/polar pocket regions proposed to contact HLA-DR1 are on opposite surfaces of Spe-C (Fig. 1).

We next examined two sets of mutants that targeted the sites shown to be important for binding of Spe-C to the MHCII α-chain, based on our modeling results. The first set, Y76A and Y87A, were mutations of residues in the polar pocket, and the second, S32A, T33A, T34A, and H35A, consisted of the hydrophobic loop mutations. Changes in position 76 of Spe-C were predicted to affect T-cell stimulation by influencing the positioning of Spe-C in the ternary superantigen/MHCII/TCR complex. The Spe-C side chain of His^{35}, homologous to Phe^{47} of SEB, in the Spe-C/DR1 model is within 4 Å of the Ala^{37} and Met^{36} side chains of DR1 α-chain. The interaction is dominated by hydrophobic contacts with the side chain of Met^{36} and the Met^{36}-Ala^{37} peptide backbone. Mutation of these hydrophobic residues was anticipated to diminish binding to MHCII. The SEB loop residues Phe^{44} and Tyr^{46} do not have structural equivalents in Spe-C. Overall, Ala replacements in the putative α-chain-binding site in Spe-C had minimal effects on protein secondary structure (data not shown) and thermodynamic stability (Table VI). The Y87A protein had slightly lower thermodynamic stability. The residue 87 in Spe-C is very conserved in

TABLE VI
Thermodynamic parameters for equilibrium unfolding of Spe-C mutant proteins

Protein concentration was 0.817 μM in 50 mM potassium phosphate, pH 7.0. Thermodynamic parameter values are average ± S.E. of two-five independent measurements.

Spe-C	ΔG^o	C_m	m
	kJ/mol	*M*	*kJ mol^{-1}M^{-1}*
r wt	31.5 ± 2.1	1.16 ± 0.04	27.2 ± 2.6
H35A	24.1 ± 8.2	1.04 ± 0.04	20.5 ± 1.2
T34A	39.0 ± 14.8	1.18 ± 0.04	43.1 ± 17.3
T33A	31.7 ± 5.9	1.03 ± 0.05	31.0 ± 6.3
S32A	35.5 ± 8.4	1.25 ± 0.02	27.7 ± 6.0
Y76A	23.0 ± 3.7	1.00 ± 0.08	23.0 ± 1.8
Y87A	14.7 ± 0.3	0.82 ± 0.07	18.0 ± 1.9

TABLE VII
A summary of affinities of recombinant HLA-DR1 for Spe-C protein variants as measured by surface plasmon resonance

The rate constants were determined at 37 °C in 10 mM HEPES, pH 7.0, 150 mM NaCl. The equilibrium dissociation constant for wt, determined from the plot of apex of the on-rates versus DR1 concentration, was between 1 and 2 μM. The value did not change when 10 mM potassium phosphate, pH 7.0, was used instead of the HEPES buffer. The data for wt protein was included for comparison.

Protein	$k_{on} \cdot 10^3$	$k_{off} \cdot 10^{-3}$	K_d	$\Delta\Delta G^o$
	1/Ms	*1/s*	*μM*	*kJ/mol*
wt	2.74 ± 0.02	2.74 ± 0.12	1.0 ± 0.05	0
S32A	1.04 ± 0.01	3.96 ± 0.21	3.82 ± 0.23	11.1 ± 0.67
T33A	0.405 ± 0.005	5.59 ± 0.13	13.8 ± 0.55	21.8 ± 0.87
T34A	0.737 ± 0.007	5.84 ± 0.13	7.9 ± 0.24	17.2 ± 0.52
H35A	0.401 ± 0.006	1.84 ± 0.23	4.6 ± 0.64	12.7 ± 1.8
Y76A	1.17 ± 0.01	4.17 ± 0.17	3.56 ± 0.18	10.6 ± 0.53
Y87A	2.09 ± 0.01	3.36 ± 0.09	1.61 ± 0.05	3.96 ± 0.12

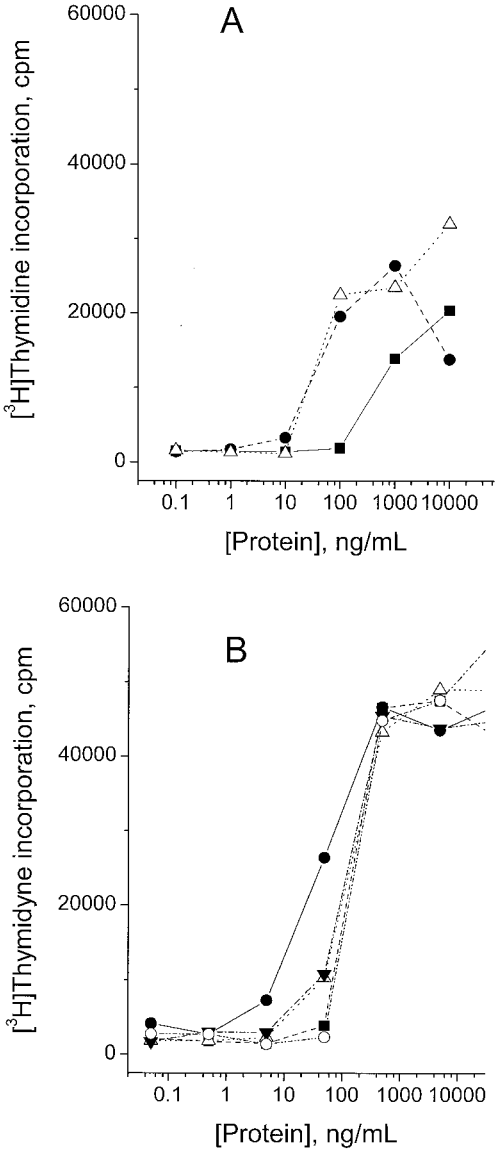

FIG. 9. **Alternative zinc-independent binding surface of Spe-C controls T-cell recognition.** *A*, stimulation of human T-cells by recombinant polar pocket mutants. ●, recombinant wild type; ▲, Y87A; ■, Y76A. *B*, stimulation of human T-cells by hydrophobic loop mutants of Spe-C. ●, recombinant wild type; ▼, S32A; △, T33A; ○, T34A; ■, H35A.

the protein structure of other bacterial superantigens (discussed later) and may form a hydrogen bond with the side chain of Ser^{182}, stabilizing an α-helix/β-sheet interaction. Replacing the Ser^{182} side chain was expected to have a negative effect on the overall stability of the protein. The replacement Y76A or Y87A had a small effect on detectable binding (Table VII). The T-cell stimulation, however, was diminished by the Y76A mutation, whereas the Y87A mutation had no effect (Fig. 9*A*). The effects of replacements in the hydrophobic loop on MHCII binding were dependent on the position (Table VII). Calculated K_ds were higher for all mutants compared with the r wt Spe-C, with the greatest effect on affinity noted for T33A and T34A. T-cell stimulation by all loop mutants was also reduced (Fig. 9*B*), the most for T34A and H35A, and slightly less for the T33A and S32A mutants. Our results clearly demonstrate that the hydrophobic loop and the polar pocket in Spe-C are important for T-cell stimulation.

DISCUSSION

Bacterial superantigens bind to MHCII receptors through one or both of two conserved sites and also to TCR molecules

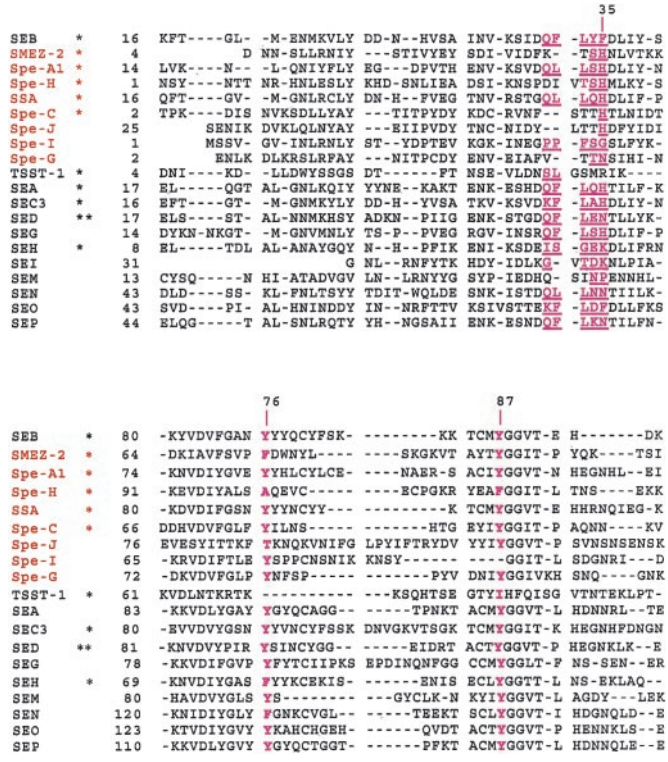

FIG. 10. **Structural alignment of known and predicted bacterial superantigen sequences in the vicinity of the MHCII α-chain binding residues of SEB protein.** *Top*, the hydrophobic loop region. *Bottom*, the polar pocket region. For clarity, only the residues structurally equivalent to Spe-C Tyr^{76} and Tyr^{87} are colored in *magenta*. The α-C backbones of structures were overlaid with Swiss PDB Viewer v.3.7 (b2) (26) program, and residues within 4 Å root mean square deviation of the corresponding amino acids of α-chain binding loop of SEB are colored in *magenta* and *underlined* (*top*) or colored in *magenta* only (*bottom*). *Numbers* on the *top* of alignments refer to residues in Spe-C protein. The sequence names corresponding to *S. pyogenes* superantigens are marked in *red*. The structures were either modeled by Swiss Model as described under "Materials and Methods" or downloaded from a PDB data base (marked with an *asterisk* by the name). The proteins and the corresponding PDB codes are as follows: SMEZ-2, 1EU3; SEB, 1SEB; Spe-H, 1EU4; SSA, 1BXT; TSST-1, 2QIL; SEA, 1SXT; SEH, 1HXY; SEC3, 1JCK; and Spe-A1, 1B1Z. **, structure of SED was solved (33), but the coordinates were not publicly available. Therefore, a model of SED was built as described under "Materials and Methods." Sequences for the modeled *S. pyogenes* proteins were derived from the Genome Sequence Data base (accession number AE004092) as described by Ferretti *et al.* (34). Accession codes for other modeled proteins were as follows: SED (AAB06195), SEG (BAB42910), SEI (AAC26661), SEJ (AAC78590), S.E. (AAG36952), SEN (AAG36956), SEO (AAG36951), and SEP (BAB43036).

through more variable sites (1). Dimerization of Spe-C was proposed previously (2) to bury the potential MHCII α-chain-binding site in the subunit interface, resulting in interaction with only the MHCII β-chain, a mechanism for binding to MHCII that differs considerably from all other superantigens. In the present study, mutation of the Cys^{27} to Ser eliminated potential covalent dimerization, without altering biological activity. Although we detected only a low proportion of dimer, superantigen interaction with surface-bound MHCII molecules may be conducive to aggregate formation. Clarification of the biologically active unit on the cell surface awaits further study. Nonetheless, our results suggest that the zinc-mediated interactions between Spe-C and MHCII observed in the x-ray structure of a co-complex (3) may reflect conditions conducive for crystallization but not necessarily the mode of interaction required for TCR signal transduction. In our study, binding of Spe-C to MHCII was greatly diminished when the zinc binding residues of Spe-C were replaced by alanines. Although these

mutations caused a minor change in ΔG^o, the Spe-C mutants retained T-cell stimulatory activity. In a previous report (18), Ala replacements of zinc binding residues in SEE/SED caused a significant decrease in thermal stability of the mutant proteins and abolished T-cell recognition, indicating an important role for zinc in stabilizing protein folding of some superantigens.

To search for a potential zinc-independent binding mode for Spe-C, we first analyzed the structural features of superantigen protein surfaces known or suggested to be involved in MHCII and TCR binding. The zinc-binding site is structurally conserved in many superantigens, as is the overall superantigen fold. Based on the available x-ray data, we constructed homology models of other zinc-binding superantigens for which the experimental data for the structure of these proteins was not available. A structural alignment extracted from these superimposed models is presented in Fig. 10. Mutation of the hydrophobic loop region in several superantigens inhibits binding to MHCII molecules (15).[2] For superantigens that are hypothesized to use an MHCII binding mechanism differing from SEB, *i.e.* are not known to insert into the hydrophobic binding surface of DR1, either the loop has a different conformation than in SEB, for example Spe-C, or it is occupied by small/non-hydrophobic residues, for example those found in Spe-G, Spe-J, Spe-H, and SMEZ-2 (Fig. 10). The zinc-binding site and polar pocket residues appear to be conserved when the hydrophobic binding loop is defective. The loop of Spe-C, alone or in conjunction with other structurally conserved residues, may be involved in a low affinity binding to MHCII molecules. However, because the structural composition of the loop is not optimal for the α-chain binding in the mode observed in SEB/MHCII complex (19), either the surface of the superantigen/MHCII interface differs, as suggested for the SSA/HLA-DQ complex (20), or the relative orientation of the MHCII and superantigen molecules differs from the SEB/MHCII complex, as observed in TSST-1/DR1 complex (21). The hydrophobic loop residue His^{35} and polar pocket residues Tyr^{76} and Tyr^{87} of Spe-C are very conserved in all *S. pyogenes* superantigens (Fig. 10). The His^{35} residue in Spe-C may contribute to the polar pocket through its proximity to the residue Glu^{54} (Fig. 8*A*). In addition, the lower free energy of unfolding for the H35A mutation (Table V) indicates that His^{35} stabilizes the loop structure. The residues structurally equivalent to Thr^{34} of Spe-C in other *S. pyogenes* superantigens (Fig. 10) are Thr (Spe-C, Spe-G, Spe-J) or Ser (Spe-I, Spe-H, Smez-2, Spe-A), possessing both hydrophobic and polar qualities. The Thr^{33} residue is involved in stabilizing the loop through intramolecular H-bonds, hence the T33A change may destabilize the loop. The replacement S32A may affect the conformation of the loop by removing a potential H-bond interaction with carbonyl oxygen from the Glu^{31}-Ser^{32} peptide bond. Both changes have a negative effect on the productive binding to DR1 leading to T-cell activation as observed in our current work (Fig. 9*B*).

In the polar pocket of Spe-C, the Tyr^{76} and Tyr^{87}, together with Glu^{54}, are proposed to bind to Lys^{39} of α-chain of DR1 (Fig. 8*B*). The residues are highly conserved in other superantigens (Fig. 10), and structurally equivalent residues are either observed to form a H-bond with Lys^{39} of α-chain of DR1 in SEB/MHCII (19) complex or postulated to form such a bond in the SEA/MHCII (16) complex model. The Y76A replacement decreased T-cell stimulation (Fig. 9*A*) whereas the mutation Y87A had no effect. In SEA, the mutation Y108A, structurally equivalent to the Y87A mutation in Spe-C, also had no effect on HLA-DR1 binding (16). However, the Y92A mutation in SEA, structurally equivalent to the Y76A mutation in Spe-C, decreased both DR1 binding and T-cell stimulation (16). The striking similarity in results obtained with both superantigens suggests that MHCII binding by the Y76A mutant of Spe-C was also diminished but masked by the dominant zinc-dependent interactions with MHCII β-chain. An alternative explanation is that the mutation Y76A, but not Y87A, has altered TCR interactions with the Spe-C/MHCII complex. However, TCR contacts with this surface of Spe-C also precludes the active role of a Spe-C homodimer as observed by Li *et al.* (3). Last, stability of the homodimer may have been affected by the mutations studied, yet dimer stability is not likely to have an influence T-cell stimulation, as the reported K_ds for dimer formation by wt and H35A mutant proteins (3) are several orders of magnitude above the physiologically relevant Spe-C concentration.

In summary, our experimental results clearly demonstrate a diminished role of zinc and dimerization in the biological activity of Spe-C. The high affinity, zinc-binding site may be important for Spe-C binding to MHCII molecules but not directly for T-cell stimulation. The zinc-dependent affinity may serve as a mechanism to increase the local superantigen concentration (16), mimicking the effect achieved by receptor oligomerization (23). A second site is proposed to be involved directly in T-cell stimulation by positioning Spe-C on the MHCII surface for biologically relevant activity, facilitating superantigen alignment in the Spe-C/MHCII/TCR ternary complex.

[2] R. G. Ulrich, unpublished results.

REFERENCES

1. Li, H., Llera, A., Malchiodi, E. L., and Mariuzza, R. (1999) *Annu. Rev. Immunol.* **17,** 435–466
2. Roussel, A., Anderson, B. F., Baker, H. M., Fraser, J. D., and Baker, E. N. (1997) *Nat. Struct. Biol.* **4,** 635–643
3. Li, Y., Li, H., Dimasi, N., McCormick, J., Martin, R., Schuck, P., Schlievert, P. M., and Mariuzza, R A. (2001) *Immunity* **14,** 93–104
4. Arcus, V. L., Proft, T., Sigrell, J. A., Baker, H. M., Fraser, J. D., and Baker, E. N. (2000) *J. Mol. Biol.* **299,** 157–168
5. Sundstrom, M., Abramsen, L., Antonsson, P., Mehindate, K., Mourad, W., and Dohlsten, M. (1996) *EMBO J.* **15,** 6832–6840
6. Petersson, K., Håkanson, M., Nilsson, H., Forsberg, G., Svensson, L. A., Liljas, A., and Walse, B. (2001) *EMBO J.* **20,** 3306–3312
7. Li, P.-L., Tiedemann, R. E., Moffat, S. L., and Fraser, J. D. (1997) *J. Exp. Med.* **186,** 375–383
8. Proft, T., Moffat, S. L., Berkahn, C. J., and Fraser, J. D. (1999). *J. Exp. Med.* **189,** 89–101
9. Proft, T., Arcus, V. L., Handley, V., Baker, E. N., and Fraser, J. D. (2001) *J. Immunol.* **166,** 6719–6719
10. Nilsson, H., Björk, P., Dohlsten, M., and Antonsson, P. (1999) *J. Immunol.* **163,** 6683–6693
11. Bavari, S., and Ulrich, R. G. (1995) *Infect. Immun.* **63,** 423–429
12. Chi, Y. I., Sadler, I., Jablonski, L. M., Callantine, S. D., Deobald, C. F., Stauffacher, C. V., and Bohach, G. A. (2002). *J. Biol. Chem.* **277,** 22839–22846
13. Sundberg, E. J., Li, H., Llera, A. S., McCormick, J. K., Tormo, J., Schlievert, P. M., Karjalainen, K., and Mariuzza, R. A. (2002) *Structure* **10,** 687–699
14. Fagin, U., Hahn, U., Grötzinger, J., Fleischer, B., Gerlach, D., Buck, F., Wollmer, A., Kirchner, H., and Rink, L. (1997) *Infect. Immun.* **65,** 4725–4733
15. Dowd, J. E., Karr, R. W., and Karp, D. R. (1996) *Mol. Immunol.* **33,** 1267–1274
16. Ulrich, R. G., Bavari, S., and Olson, M. A. (1995) *Nat. Struct. Biol.* **2,** 554–559
17. Papageorgiu, A. C., Collins, M. C., Gutman, D. M., Kline, J. B., O'Brien, S. M., Tranter, H., S., and Acharya, K. R. (1999). *EMBO J.*, **18,** 9–21
18. Cavallin, A., Arozenius, H., Kristensson, K., Antonsson, P., Otzens, D. E., Björk, P., and Forsberg, G. (2000) *J. Biol. Chem.* **275,** 1665–1667
19. Jardetzky, T. S., Brown, J. H., Gorga, J. C., Stern, L. J., Urban, R. G., Chi, Y. I., Stauffacher, C., Strominger, J. L., and Wiley, D. C. (1994) *Nature* **368,** 711–718
20. Sundberg, E., and Jardetzky, T. S. (1999) *Nat. Struct. Biol.* **6,** 123–129
21. Kim, J., Urban, R. G., Strominger, J. L., and Wiley, D. C. (1994) *Science* **266,** 1870–1874
22. Seth, A., Stern, L. J., Ottenhoff, T. H., Engel, I., Owen, M. J., Lamb, J. R., Klausner, R. D., and Wiley, D. C. (1994) *Nature* **369,** 324–327
23. Bachmann, M. F., and Ohashi, P. S. (1999) *Immunol. Today* **20,** 568–576
24. Sloan, V. S., Cameron, P., Porter, G., Gammon, M., Amaya, M., Mellins, E., and Zaller, D. M. (1995) *Nature* **375,** 802–806
25. Stern, L. J., Brown, J. H., Jardetzky, T. S., Gorga, J. C., Urban, R. G., Strominger, J. L., and Wiley D. C. (1994) *Nature* **368,** 215–221
26. Guex, N., and Peitsch, M. C. (1997) *Electrophoresis* **18,** 2714–2723
27. Rodriguez, R., Chinea, G., Lopez, N., Pons, T., and Vriend, G. (1998) *Comput. Appl. Sci.* **14,** 523–528
28. Willet, P. (1995) *Trends Biotechnol.* **13,** 516–521

29. Meegan, M. J., Hughes, R. B., Lloyd, D. G., Williams, C. D., and Zisterer, D. M. (2001) *J. Med. Chem.* **44,** 1072–1084
30. Dhar, A., Liu, S., Klucik, J., Berlin, D., Madler, M. M., Lu, S., Ivey, R. T., Zacheis, D., Brown, C., Nelson, E. C., Birkbichler, P. J., and Benbrook, D. M. (1999). *J. Med. Chem.* **42,** 3602–3614
31. Bertelli, M., El-Bastawissy, E., Knaggs, M. H., Barrett, M. P., Hanau, S., and Gilbert, H. (2001) *J. Comput. Aided Mol. Des.* **15,** 465–475
32. Clark, M., Cramer, R. D., III, and Opdenbosch, N. V. (1989) *J. Comp. Chem.* **10,** 982–1012
33. Sundstrom, M., Abramsen, L., Antonsson, P., Mehindate, K., Mourad, W., and Dohlsten, M. (1996) *EMBO J.* **15,** 682–40
34. Ferretti, J., McShan, W. M., Ajdic, D., Savic, D. J., Savic, G., Lyon, K., Primeaux, C., Sezate, S., Suvorov, N., Kenton, S., Lai, H. S., Lin, S. P., Qian, Y., Gia, H. G., Najar, F. Z., Ren, Q., Zhu, H., Song, L., White, J., Yuan, X., Clifton, S., Roe, B. A., and McLaughlin, R. (2001) *Proc. Natl. Acad. Sci. U. S. A.* **98,** 4658–4663